Phase diagram of the mixed crystals betaine phosphate and betaine phosphite: Experimental and Monte Carlo results

J. Banys
Universität Leipzig, Fakultät für Physik und Geowissenschaften, D-04103 Leipzig, Germany

P. J. Kundrotas
Department of Physics/Theoretical Physics, The Royal Institute of Technology, S-100 44 Stockholm, Sweden and Faculty of Physics, Vilnius University, Sauletekio al. 9, LT-2040 Vilnius, Lithuania

C. Klimm
Universität Leipzig, Fakultät für Physik und Geowissenschaften, D-04103 Leipzig, Germany

A. Klöpperpieper
Fachbereich Physik, Universität des Saarlandes, D-66123 Saarbrücken, Germany

G. Völkel
Universität Leipzig, Fakultät für Physik und Geowissenschaften, D-04103 Leipzig, Germany
(Received 4 May 1999; revised manuscript 8 September 1999)

We propose a microscopic model that is capable of describing the features of both deuterated and nondeuterated betaine phosphate (BP)–betaine phosphite (BPI) solid solutions in the region of small concentration of BP. The size mismatch between the BP and BPI structural units, which leads to a drastical change of the nearest-neighbor interactions in the vicinity of single BP impurity, was taken into account in the model. We show that the model quite accurately reproduces the experimentally observed abrupt drop of the ferroelectric phase transition temperature. The onset of the glass state given by the model also agrees well with the experimental results.

Substitution of one structural unit by another similar unit may in some crystals drastically change properties of the parent compound toward either an improvement or deterioration of desired features. An impressive example of such a system is the solid solution of betaine phosphate [BP:$(CH_3)NCH_2COOH_3PO_4$] and betaine phosphite [BPI: $(CH_3)NCH_2NCOH_3PO_3$]. Both compounds are molecular crystals of the amino acid betaine and phosphoric (BP) and phosphorous (BPI) acids and contain inorganic components (PO_3 or PO_4 tetrahedral groups) linked by hydrogen bonds forming zig-zag chains along the monoclinic b axis[1] [Fig. 1(a)]. The two almost isostructural compounds form solid solutions at any proportions,[2] which makes the BP_xBPI_{1-x} system ($0 \leqslant x \leqslant 1$) a convenient object for both experimental and theoretical fundamental studies.

Both BP and BPI exhibit a phase transition from a paraelectric high-temperature phase with space group $P21/m$ to an antiferrodistortive phase with space group $P21/c$ at 365 K (BP)[1] and 355 K (BPI).[1,2] The high-temperature phase of both compounds is characterized by disorder of the hydrogen atoms as well as of orientations of both tetrahedra and betaine molecules, which order in the antiferrodistortive phase while the hydrogen atoms between the PO_3 or PO_4 group remain disordered. There are two further structural phase transitions in BP, one at 86 K into an intermediate phase with the $P21$ symmetry, and the other at 81 K into a low-temperature phase with doubling of the unit cell along the crystallographic a direction.[3] *Antiferroelectric* order is claimed to occur at $T_c = 86$ K,[4] but there exist some doubts about this.[3] BPI exhibits below $T_c = 216$ K a *ferroelectric* ordered phase with space group $P2_1$.[1,2] The hydrogen atoms order below T_c within the double-well potential of the O−H $\cdots$O bonds between the PO_3 (PO_4) groups and spontaneous polarization of the chain occurs. In BP neighboring chains have opposite direction of polarization,[5] while in BPI the chains have the same direction of the polarization.

The BP_xBPI_{1-x} system was extensively studied experimentally[6–11] and it is clearly established that the low-temperature part of the (T,x) phase diagram of the BP_xBPI_{1-x} system consists mainly of (i) a ferroelectric phase for $0 \leqslant x \lesssim 0.1$, (ii) an antiferroelectric phase for $0.65 \lesssim x \leqslant 1$, and (iii) so-called glass phase for $0.1 \lesssim x \lesssim 0.65$, where the proton motion is frozen out below a certain temperature leading to a disordered array of asymmetrically occupied O−H$\cdots$O bonds. The phase diagrams for the solid solutions of both nondeuterated BP_xBPI_{1-x} and deuterated DBP_xDBPI_{1-x} are shown in Fig. 2. The main difference between the two systems is the discrepancy in the absolute values of the phase transition temperatures T_c, which are higher for DBP_xDBPI_{1-x} within the whole interval of x. Both compounds show an abrupt decrease in T_c at small x with ferroelectricity completely destroyed at $x \gtrsim 0.1$. Contrary to that, antiferroelectric ordering persists within a much wider x range ($0.7 \lesssim x \leqslant 1$). The similarity in the behavior of both systems manifests itself even more clearly if the phase diagram is plotted using a normalized temperature T_c/T_c^{max} (where T_c^{max} is T_c at $x=0$ for the BP_xBPI_{1-x} and

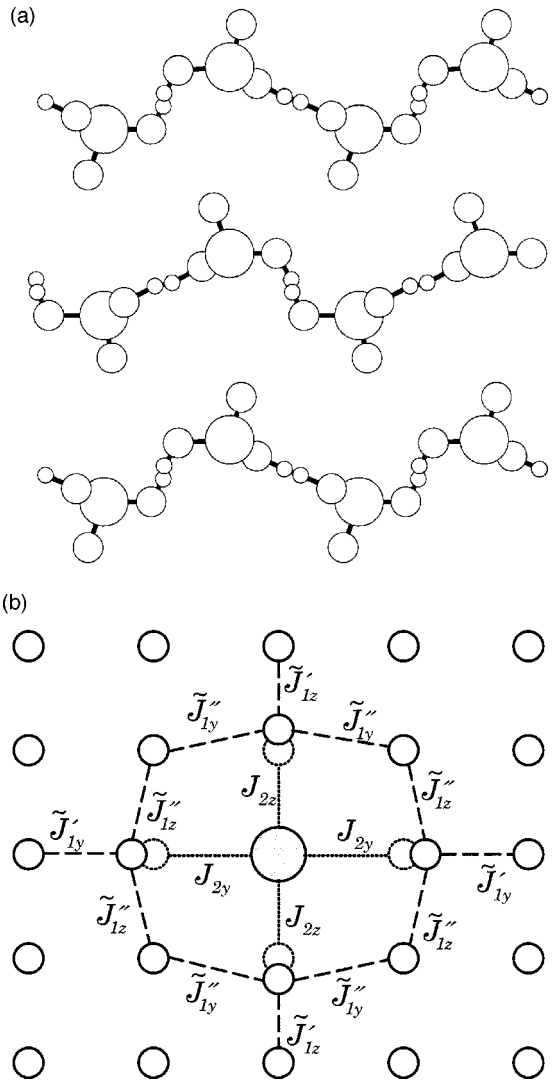

FIG. 1. Schematic representation of the hydrogen chains in the *c*-*b* crystallographic plane for the BPI (a) and schematic representation of a distortion in the system of Ising pseudospins caused by the presence of a single impurity (b). Large open circles in (a) denote phosphorus atoms, oxygen (position for hydrogen) atoms are pictured as middle (small) open circles. The impurity in (b) is shown as the large circle and dashed circles show the positions of pseudospins in the absence of impurity. For the notation of interaction constants see the text.

DBP_xDBPI_{1-x} systems, respectively) as shown in the inset of Fig. 2. Therefore, the ferroelectric features of both systems might be described within the framework of a general microscopic model.

The considerable increase in T_c when hydrogen in hydrogen-bonded ferrolectrics is replaced by deuterium was recently described within the framework of a model, which takes into account the bilinear coupling between the tunneling protons and the displacements of the electron shells of the neighboring PO_4 groups.[12] However, this model does not describe changes of T_c due to the substitution of other structural elements, e.g., PO_3 groups with the PO_4 ones. Due to the chainlike fashion in the arrangement of the hydrogen bonds, betaines (hereafter we mean both deuterated and nondeuterated systems) are potential candidates for the application of quasi-one-dimensional models.[13,14] The anisotropic

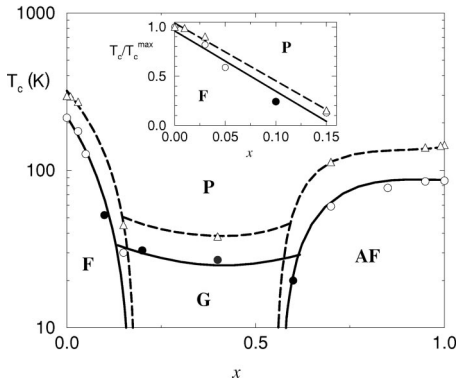

FIG. 2. The (T,x) phase diagram of the solid solutions of BP_xBPI_{1-x} (represented by circles) and DBP_xDBPI_{1-x} (drawn by triangles). **F**, **AF**, **G**, and **P** denote the ferroelectric, antiferroelectric, spin-glasses, and paraelectric phases, respectively. Inset shows the **F-P** part of the phase diagram plotted using normalized temperature. Solid (for BP_xBPI_{1-x}) and dashed (for DBP_xDBPI_{1-x}) lines are guides to the eye. Open symbols represent the experimental results obtained by the authors of the present paper from the dielectric measurements at the frequency 100 Hz and filled symbols are the data taken from Ref. 8.

Ising model with nearest neighbor (NN) interactions might thus serve as a simplest microscopic model for the betaines. The Hamiltonian of this model is

$$\mathcal{H}=-J_z\sum_{ij}\ \sigma_{ij}\sigma_{i\pm 1j}-J_y\sum_{ij}\ \sigma_{ij}\sigma_{ij\pm 1}, \qquad (1)$$

where σ_{ij} is an Ising pseudospin (hereafter, spin) that equals ± 1 depending on which position of the double-well potential hydrogen occupies. Indices i and j number spins along and across the chains, respectively, and J_z and J_y are the interactions between spins along the i and j axis, respectively. At $x=0$ $J_z>0$ and $J_y>0$, while at $x=1$ $J_z>0$ and $J_y<0$.

In order to describe the system at any x each interaction J_z and J_y should be further split into three components J_{1z}, J_{2z}, J_{3z}, and J_{1y}, J_{2y}, J_{3y}, where indices 1, 2, 3 denote interactions between the hydrogen atoms located between the PO_3 groups in the chain (BPI units), between the PO_3 and PO_4 groups (BPI and BP units), and between the PO_4 groups (BP units), respectively. Ferroelectric ordering along the chains persists at both ends of the phase digram and therefore one can take $J_{1z}=J_{2z}=J_{3z}=J_z>0$. The asymmetry of the phase diagram implies that $J_{2y}<0$. Then, a single BP unit (hereafter referred to as impurity) surrounded by BPI units locally destroys ferroelectric order while at large x antiferroelectricity is locally destroyed only if there are several neighboring BPI units. The Hamiltonian of the model could thus be written as

$$\mathcal{H}_1=-J_z\sum_{ij}\ \sigma_{ij}\sigma_{i\pm 1j}-J_{1y}\sum_{BPI-BPI}\ \sigma_{ij}\sigma_{ij\pm 1}$$

$$-J_{2y}\sum_{BPI-BP}\ \sigma_{ij}\sigma_{ij\pm 1}-J_{3y}\sum_{BP-BP}\ \sigma_{ij}\sigma_{ij\pm 1}. \qquad (2)$$

The model (2) is the simplest model applicable to the betaine systems if one wants to calculate quantities of interest for the

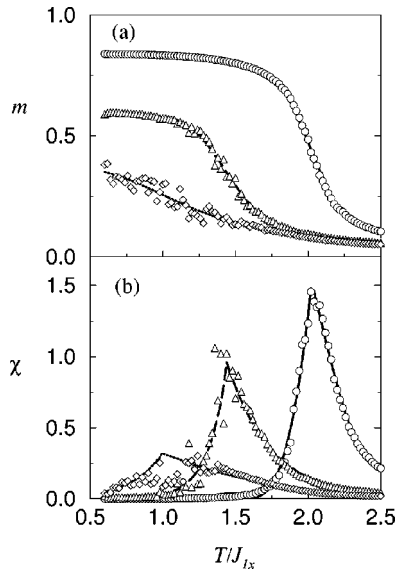

FIG. 3. Temperature variations of the magnetization m (a) and of the susceptibility (b) of the system described by the Hamiltonian (3) at different concentration x of impurities. Circles represent the results of simulations at $x=0.03$, triangles show results for $x=0.07$ and diamonds stand for the results at $x=0.10$. All the data points shown in the figure are obtained on the 32×32 lattice from the average over number of runs (varied from 3 to 7) with different random distribution of impurities, each of 100 000 MCS/S. Solid ($x=0.03$), dashed ($x=0.07$), and dotted ($x=0.1$) lines are guides for the eye.

BP_xBPI_{1-x} and DBP_xDBPI_{1-x} systems. It should be noted, that results of calculations do not depend in an essential way either on whether a two- or three-dimensional model is used for the calculations or on the ratio (within a wide range) of the interaction constants, and henceforth, for the sake of simplicity, we restrict ourselves to the two-dimensional case with $|J_z|=|J_{1y}|=|J_{2y}|=|J_{3y}|$. We performed Monte Carlo calculations of the model (2) and found, however, that the model has serious drawbacks. For instance, at $x=0.1$ the model predicts $T_c/T_c^{max}\sim0.8$, while experiment gives $T_c/T_c^{max}\sim0.25$.

In order to describe the experimental data we propose the following modification of the model (2). Due to size mismatch between PO_4 and PO_3 groups, BPI units in the neighborhood of a single BP impurity are shifted from their equilibrium positions [Fig. 1(b)]. It is plausible then to suppose that a BP unit changes the interaction between neighboring BPI units also and since four BPI units experience the largest shift, we take into consideration six changed interactions J_{1y} (denoted as $\tilde{J}'_{1y}$ and $\tilde{J}''_{1y}$). Then

$$\mathcal{H}=\mathcal{H}_1-\tilde{J}'_{1y}\sum_{i'j'}\sigma_{i'j'\pm1}\sigma_{i'j'\pm2}-\tilde{J}''_{1y}\sum_{i'j'}\sigma_{i'\pm1j'}\sigma_{i'\pm1j'\pm1}, \tag{3}$$

where i',j' denote positions of the BP impurities and $\mathcal{H}_1$ is the Hamiltonian (2) taken over the whole lattice except the nearest surrounding of impurities. Under above described assumptions the model proposed reduces to the simple two-dimensional Ising model with NN interactions where the presence of an impurity is described by introducing *two* additional parameters. One of them is the change of the ''original'' NN interactions in the immediate surrounding of the impurity and another is the change of ''original'' interactions in the more distant neighborhood of the impurity.

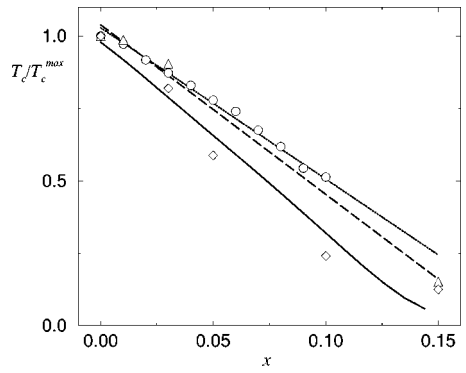

FIG. 4. The comparison of the **F-P** transition lines obtained from the MC (circles, dotted line) calculations and from the experimental results for the BP_xBPI_{1-x} (diamonds, solid line) and DBP_xDBPI_{1-x} (triangles, dashed line) systems. Lines are guides for the eye.

We employed the Metropolis Monte Carlo algorithm with Glauber dynamics[15] in order to calculate the (T,x) phase diagram of the model (3) for $x\leqslant0.15$. Most of our results were obtained on a 32×32 square lattice with periodic boundary conditions. Data points were averaged over 100 000 Monte Carlo steps per lattice site (MCS/S) after the system reached equilibrium. To make sure that finite size effects do not affect our results we also performed several runs on larger lattices (up to 128×128). At each MCS/S we calculated the magnetization m of the system $m=(1/N)\Sigma_{ij}\sigma_{ij}$, and the susceptibility $\chi=(1/T)(\langle m^2\rangle-\langle m\rangle^2)$ with N being the number of particles in the system and $\langle\ldots\rangle$ denoting the average over MCS/S. The T_c's were determined from the position of the maxima in the $\chi(T)$ dependence.

For the sake of simplicity we restrict ourselves to the case $\tilde{J}'_{1y}=\tilde{J}''_{1y}=\tilde{J}_{1y}$ and performed calculations varying the *only* parameter $\tilde{J}_{1y}$ in a wide range with respect to J_{1y}. We find the best agreement with experiment for $\tilde{J}_{1y}=-J_{1y}$ which means an amplification of the antiferroelectric character of a BP impurity in BPI. Results for m and χ with this choice of parameters are shown in Fig. 3 for three values of x. As seen, for $x<0.1$ m and χ show a behavior typical for an order-disorder phase transition with T_c decreasing with increasing x. Contrary to that for $x\geqslant0.1$ the magnetization does not reach saturation down to the lowest temperatures we were able to calculate and the results are very scattered, i.e., the dynamics of the system becomes very slow. The peak in $\chi(T)$ disappears almost completely at $x=0.1$. We think that at $x\gtrsim0.1$ our system starts exhibiting glasslike behavior when spins remain disordered with their dynamics being extremely slow. Indeed, when x is sufficiently large the model (3) might be viewed as the so-called, Edwards-Anderson model, a model with random alternation of ferromagnetic and antiferromagnetic NN bonds, usually used to describe spin-glasses.[16,17] Note, that the onset of the glassy state predicted by our model agrees well with the experimental estimate $x=0.1-0.15$ (see Fig. 2). The (T,x) phase diagram

obtained for small x is plotted in Fig. 4 along with the experimental data for the BP_xBPI_{1-x} and DBP_xDBPI_{1-x} compounds. One can see that our model describes quite well the behavior of both systems. Note, that for the DBP_xDBPI_{1-x} system the agreement between theory and experiment is better than that for the BP_xBPI_{1-x} system. We think this is due to the fact that our model does not take into consideration such a phenomenon as proton tunneling, recently observed in the $BP_{0.15}BPI_{0.85}$ compound.[18]

One may ask, what the physical reason is for such a seemingly drastic change of the interactions between the BPI units in the neighborhood of BP unit, especially with respect to the fact that distances between the atoms in both BPI and BP differ slightly only (e.g., the distance between PO_3 groups in BPI is 3.75 Å and the distance between PO_4 groups in BP is 4.0 Å)? In the pure BPI there is an alternation of the hydrogen bonds parallel and almost perpendicular to the b axis [Fig. 1(a)], while in the pure BP compound the presence of the extra oxygen atom rearranges the hydrogen bonds in such a way that the angle between the bond and the b axis becomes the same for all the bonds. Then, a lonely BP unit surrounded by the BPI units introduces an effective strain field which in turn distorts the symmetric shape of double-well potential of a hydrogen bond in the neighborhood of the impurity. Such a distortion may lead to the situation when it becomes energetically favorable for the neighboring hydrogen atoms across the chains to occupy different positions of the double-well potential. This, in the language of the Ising pseudospins, means the change in the sign of interaction constant.

We are grateful to A. Rosengren and S. Lapinskas for stimulating discussions. This work was supported by the Alexander von Humboldt Stiftung (J.B.) and by The Swedish Institute (P.K.).

[1] J. Albers, Ferroelectrics **78**, 3 (1988); G. Schaack, *ibid.* **104**, 147 (1990).
[2] J. Albers, A. Klöpperpieper, H. J. Rother, and S. Hussühl, Ferroelectrics **81**, 27 (1988).
[3] M. Lopes dos Santos, J. M. Kiat, A. Almeida, M. R. Chaves, A. Klöpperpieper, and J. Albers, Phys. Status Solidi B **189**, 371 (1995).
[4] J. Albers, A. Klöpperpieper, H. J. Rother, and K. Ehses, Phys. Status Solidi A **74**, 553 (1982).
[5] W. Schildkamp and J. Z. Spilker, Z. Kristallogr. **168**, 159 (1984).
[6] M. L. Santos, J. C. Azevedo, A. Almeida, M. R. Chaves, A. R. Pires, H. E. Müser, and A. Klöpperpieper, Ferroelectrics **108**, 363 (1990).
[7] M. L. Santos, M. R. Chaves, A. Almeida, A. Klöpperpieper, H. E. Müser, and J. Albers, Feroelectr. Lett. **15**, 17 (1993).
[8] H. Ries, R. Böhmer, and A. Loidl, Z. Phys. B: Condens. Matter **99**, 401 (1996).
[9] J. Banys, C. Klimm, G. Völkel, H. Bauch, and A. Klöpperpieper, Phys. Rev. B **50**, 16 751 (1994).
[10] J. Banys, A. Kajokas, C. Klimm, G. Völkel, and A. Klöpperpieper, J. Phys.: Condens. Matter **10**, 8389 (1998).
[11] S. L. Hutton, I. Fehst, R. Böhmer, M. Braune, B. Mertz, P. Lunkenheimer, and A. Loidl, Phys. Rev. Lett. **66**, 1990 (1991).
[12] A. Bussmann-Holder and K. H. Michel, Phys. Rev. Lett. **80**, 2173 (1998).
[13] J. D. Reger and K. Binder, Z. Phys. B: Condens. Matter **60**, 137 (1985).
[14] M. Oresic and R. Pirc, Phys. Rev. B **47**, 2655 (1993).
[15] K. Binder, *Monte Carlo Methods in Statistical Physics*, edited by K. Binder (Springer-Verlag, Berlin, 1979).
[16] S. F. Edwards and P. W. Anderson, J. Phys. F: Met. Phys. **5**, 965 (1975).
[17] S. Kirkpatrick and D. Sherrington, Phys. Rev. B **17**, 4384 (1978).
[18] G. Völkel, H. Bauch, R. Böttcher, A. Pöppl, H. Schäfer, and A. Klöpperpieper, Phys. Rev. B **55**, 12 151 (1997).